Calculation of Initial Stiffness of Semirigid Connections with Consideration of Rotational Constraint on Angle from Beam Contact Surface

X.G. Lin
Osaka Institute of Technology, Japan

K. Asada
Obayashi Corporation, Japan

SUMMARY:
The objective of this paper is to derive a new formula to improve initial stiffness calculation of semi-rigid steel beam-to-column connections with top and seat flange angles. In order to improve prediction of initial stiffness, deformation of the connection from FEM model is closely examined and some deformation characteristics are observed such as how and when angle can be separated from beam in the vicinity of bolt. Based on those observations, some mechanical assumptions are made about how horizontal arm of angle is bent and then a new initial stiffness correction factor is proposed. The initial stiffness formula is further modified to allow a small separation between angle and column at bolt locations when angle starts to fail. The new formula also includes web angle contribution. When initial stiffness calculated using the formula proposed here is compared with lab test results, most of data shows their difference remains within 10%.

Keywords: semirigid connection, high strength bolt, steel frame, initial stiffness

1. INTRODUCTION

After many weld fractures were observed in rigid (welded) connections of building structures during Hyogo- ken-Nambu Earthquake of Japan (on January 17, 1995), structural engineers are getting more and more interest in designing semi-rigid (bolted) beam-to-column connections with angle or split tee because semi-rigid connections allow more deformation and absorb more energy and can prevent possible brutal weld fracture failure given by rigid connections during an earthquake. But displacements of frames are not welcome in general and have to be calculated and controlled. So design of semi-rigidly jointed steel frames will be more challenging than design of rigidly jointed steel frames. Therefore accurate calculations of displacements or initial stiffness are needed in design of semi-rigid beam-to-column connections. In order to estimate initial stiffness of semi-rigid beam-to-column connections for displacement calculation, C.Faella(1999), N.Kishi and Wai-Fan Chen (1990) have developed and introduced several formulas for the stiffness calculation. In their work, the vertical arm of an angle (top or seat) used to be simplified as cantilever beams and deformation in horizontal direction of the vertical arms was assumed uniformed or same.

Authors of this paper has published an initial stiffness reduction factor in the past, which tries to consider deformation difference in the horizontal direction of the angles. Although the initial stiffness reduction factor is an improvement in initial stiffness calculation, but it still has following limitations: (1) the stiffness correction factor proposed earlier to consider rotational constraint on beam contact surface is determined based on averaged numerical results while it could vary from one structure to another structure; (2) earlier stiffness formula is based on assumption that failure occurs in angle instead of bolt and angle never separate from column at bolt locations; (3) earlier stiffness formula is only verified by angle tension tests; (4) earlier stiffness formula doesn't count contribution from web angle and can not be used in the connection with web angle in addition to top and seat angles.

In this study, some 3-D finite element modeling and analysis using ABAQUS are conducted. In ABAQUS nonlinear analysis the separation between angle and column or beam at bolt location is considered and also plastic deformation in angle is included. Based on numerical simulation results, a new initial stiffness correction factor is proposed and the initial stiffness formula is further modified after allowing a small separation between angle and column at bolt locations when angle starting to fail. In finite element modeling and analysis, web angle contribution is compared with top and seat angles. A new formula is derived to include web angle contribution. Before finite element modeling and analysis of different joint configurations, eight physical test specimens are built and tested. Among them, 4 are flange angle connections and 4 are web angle connections. Results calculated using the proposed initial stiffness formula is compared with bending test results and the accuracy is verified.

2. BENDING TEST OF SEMIRIGID BEAM-TO-COLUMN CONNECTION

This paper is to study application of top and seat flange angle as well as double web angle to beam-to-column connection. In order to study individual contribution of them, top and seat flange angle is used in some tests and double web angle is used in some other tests. Fig. 1 shows pictures for two typical semi-rigid beam-to-column connections. The first connection consists of two beams, one center plate and four flange angles. Column is replaced by a center plate to exclude column contribution and make study focus on angles contribution. The second connection consists of two beams, one center plate and two top flange angles and four web angles. The use of top flange angle in the second type of connection is to keep beams having the same rotation center (the top corner of beams) and has little contribution in stiffness because it is located in compressive side.

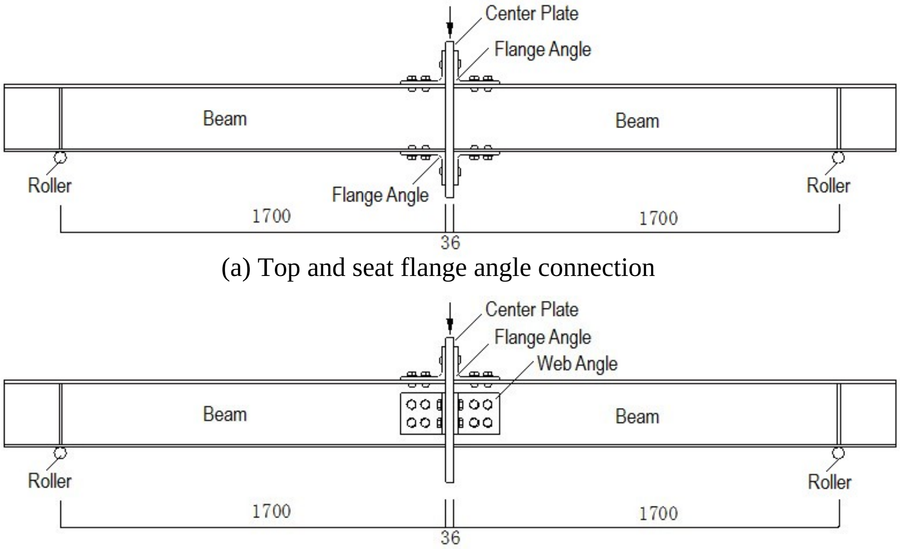

(a) Top and seat flange angle connection

(b) Double web angle connection

Figure 1. Bending test specimens

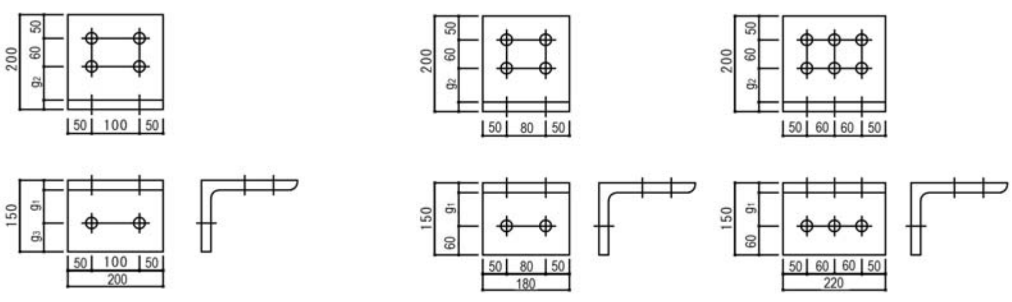

(a) Flange angle

(b) Web angle

Figure 2. Connection details for specimen of both types

Table 2.1. Details of bending test specimens

Specimen	Angle thickness (mm)	Angle width (mm)	g_1 (mm)	g_2 (mm)	g_3 (mm)	Specimen	Angle thickness (mm)	Angle Width (mm)	g_1 (mm)	g_2 (mm)
L15-70	15	200	70	75	65	WL15-2	15	180	75	75
L15-60	15	200	60	75	75	WL15-3	15	220	75	75
L20-70	20	200	70	70	60	WL20-2	20	180	70	70
L20-60	20	200	60	70	70	WL20-3	20	220	70	70

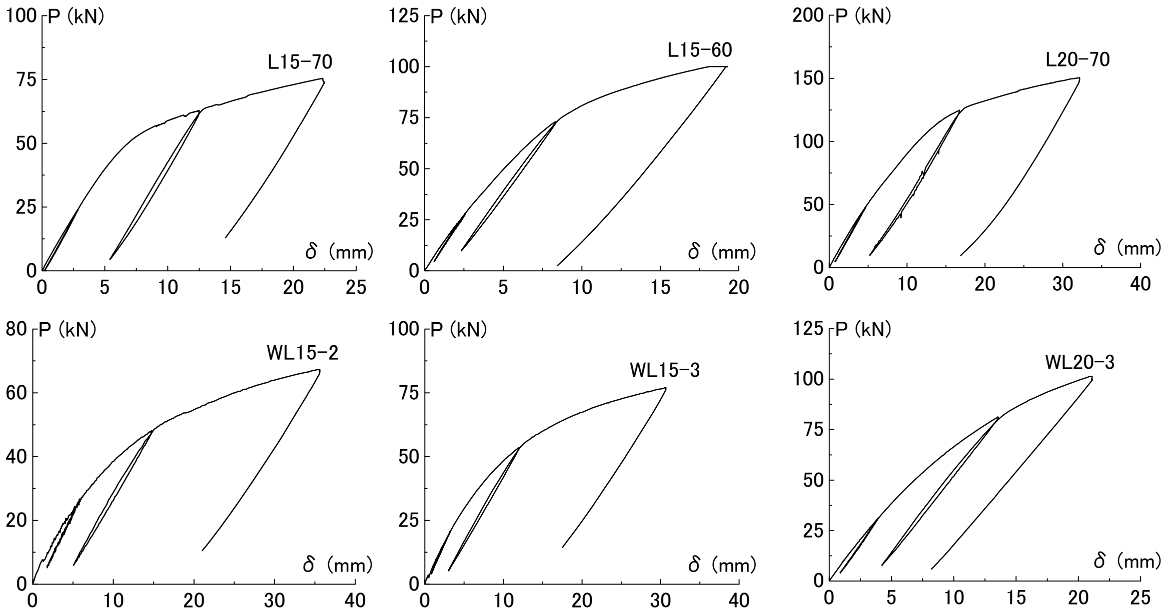

Figure 3. Load versus displacement curves for bending tests

Table 2.2. Results of bending tests

Specimen	Initial stiffness		Yield strength (kN)	Specimen	Initial stiffness		Yield strength (kN)
	Loading (kN/mm)	Unloading (kN/mm)			Loading (kN/mm)	Unloading (kN/mm)	
L15-70	920	970	58.5	WL15-2	522	510	51.8
L15-60	1208	1179	85.4	WL15-3	852	657	60.5
L20-70	1125	1125	128.8	WL20-2	839	696	65.0
L20-60	1214	1200	141.7	WL20-3	892	886	77.5

All test specimens are made of JIS steel grade SS400. Angles have two thickness of 15 mm and 20 mm. Angles are cut from either L-200x200x20 or L-200x200x15. Fig. 2 shows all major dimensions for all different angles. Beam is H-294x200x8x12. Center plate is 36 mm thick. High strength bolts are M22 of either F10T or S10T. All bolt holes have 2 mm clearance. More detailed data of all eight specimens are listed in Table 2.1.

All loading test are conducted using Amsler type universal testing machine. For each of tests, a vertical load is applied to center plate and load is increased slowly until angles deformation get into large plastic range. Beams are unloaded twice during testing. One unloading is performed in elastic range and another in plastic range. Only vertical displacement in center plate is used in stiffness calculation. Since axial force in beam is not desired, roller supports are used to give beams free moving in axial direction.

Fig. 3 presents some of typical load-deflection curves. Table 2.2 summarizes calculated initial stiffness and yield strength. In Table 2.2, initial stiffness is calculated twice. One is calculated based on elastic loading curve slope and another is based on elastic unloading curve slope. Because deflection is very small from elastic loading curve and it is not easy to measure it accurately, initial stiffness based on unloading curve is chosen for later comparison with initial stiffness prediction. The yield strength is determined using general yielding calculation. It is easily noticed that initial stiffness of each specimen depends mainly on angle thickness and number of bolts. All beams remains in elastic range. When initial stiffness is calculated using test data, beam deformation is required and it is calculated using elastic theoretical calculation instead of test measurement.

3. IMPROVEMENT OF STIFFNESS PREDICTION FOR FLANGE ANGLE CONNECTION

Fig. 4 is a picture of semi-rigid beam-to-column connection. In the past, for tensional stiffness study authors of this paper proposed mechanical mechanism illustrated in Fig. 5. Eqn. 3.1 is the tension stiffness formula developed based on this mechanism. The main feature of this formula is consideration of angle deformation in the vicinity of bolts and introduces an angle stiffness reduction coefficient in width direction.

$$K_t = a_t (B_r + \alpha_{c1} B_{f1} + \alpha_{c2} B_{f2}) K_{t0}$$
$$\alpha_c = \beta_c^{(\frac{\gamma_c}{3} - 1.4)}, \quad \beta_c = 1 + \frac{0.65 B_f}{\ell_c}, \quad K_{t0} = \frac{E\, t^3}{\ell_c^3 (1+\gamma_c)}, \quad \gamma_c = 3.12 \left(\frac{t}{\ell_c} \right)^2 \tag{3.1}$$

K_{t0} is theoretical stiffness of unit width of the rigid segment, t is thickness of the angle and E is elastic modulus of steel and γ_c is coefficient of shear deformation. B_r and ℓ_c is width and length of the rigid segment respectively. B_f is the width of the flexible segment, α_c is a stiffness reduction coefficient, which is a stiffness ratio between the rigid segment and the flexible segment with same width.

In the right end of mechanical mechanism illustrated in Fig. 5 if beam flange and angle do not separate, the right end cannot rotate and it will be similar to a fixed end. After flange and angle separate, the right end will rotate even it could get some resistance from contact surfaces. Compared with fixed end, its stiffness will be reduced. A correction factor a_t is reflecting the stiffness reduction. Authors of this paper adopted average value of numerical results of the correction factor in previous study. But different beam-to-column connection should have different correction factor. Use of average value could result in error in the calculation. In addition, rigid segment length calculation up to the front of bolt is another one required further investigation because it is only good for the failure where bolts have little deformation and angle causes the failure. When bolt stretch increases, inaccuracy will increase.

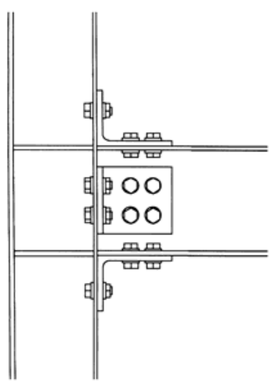

Figure 4. Semi-rigid connection

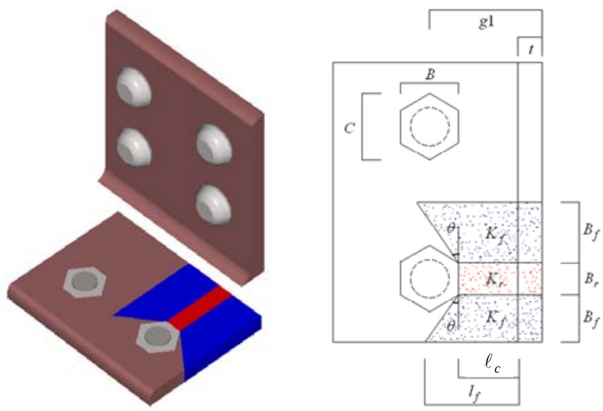

Figure 5. Segmental beam model for vertical arm of top angle

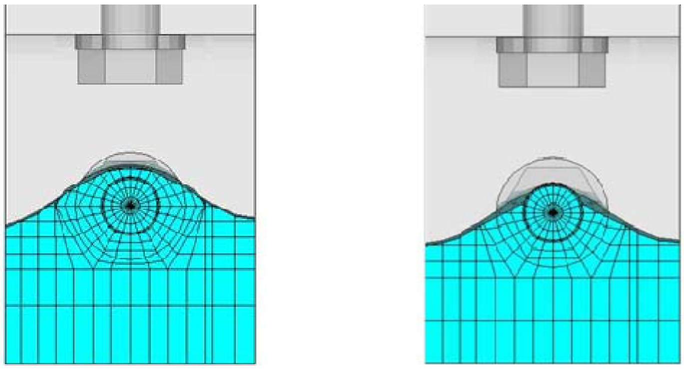

(a) L15-70 (b) L20-70

Figure 6. Separation pattern in the vicinity of bolt area

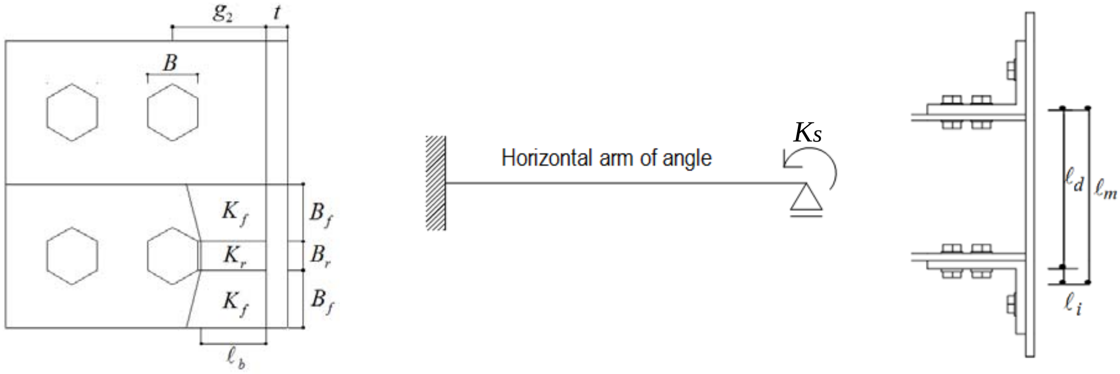

Figure 7. Segmental beam model for horizontal arm of top angle

In order to improve stiffness prediction, this paper conducts FEM modeling and analysis on test specimens and studies the way how angle deforms in the finite element models. Fig. 6 shows angle contact separation curves on the vertical arm. Compared with 15 mm thick L15-70, 20 mm thick L20-70 shows a lower separation curve, which extends into the bolt hole. In the horizontal arms, separation lines show similar trend, but they do not pass bolt holes at all and all stop in the front of bolts. In order to develop correction factor formula, rotational stiffness *Ks* is required to calculate first according to Fig. 7. Because contact separation curves are similar in the vertical arm and horizontal arm, after length ℓ_c is modified in Fig. 5, new mechanical mechanism is obtained as in Fig. 7. To use this new mechanical mechanism, rotational stiffness can be derived as follow.

$$K_s = (B_r + \alpha_{b1} B_{f1} + \alpha_{b2} B_{f2}) K_{s0}$$
$$\alpha_b = \beta_b^{(\frac{\gamma_b}{3} - 0.52)}, \quad \beta_b = 1 + \frac{0.65 B_f}{\ell_b}, \quad K_{s0} = (1 + \frac{3}{1+\gamma_b}) \frac{E t^3}{12 \ell_c}, \quad \gamma_b = 3.12\left(\frac{t}{\ell_b}\right) \tag{3.2}$$

In the above formula, $\ell_b, \alpha_b, \beta_b, \gamma_b$ are contact parameters in the horizontal arm and they have definition similar to those in Eqn. 3.1. *Ks0* is rotational stiffness of unit width of rigid segment. Formula for α_b is a simplified one and the error introduced by this simplification is bigger than same calculation in the vertical arm. To use established above, correction factor a_t can be estimated as follow.

$$a_t = \frac{1+\gamma_c}{4 + \gamma_c - \dfrac{12 + 3\gamma_b}{4 + \mu + \gamma_b + \mu\gamma_b}}, \qquad \mu = \frac{(B_a / B_b)\ell_b}{(B_a / B_c)^{1/3} \ell_c} \tag{3.3}$$

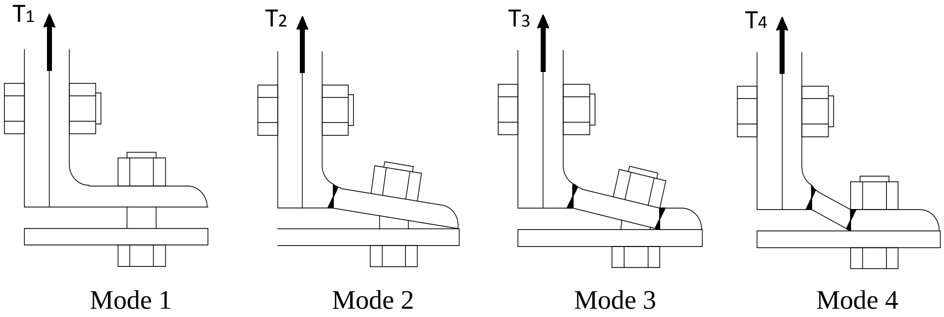

Figure 8. Failure modes for semi-rigid connection

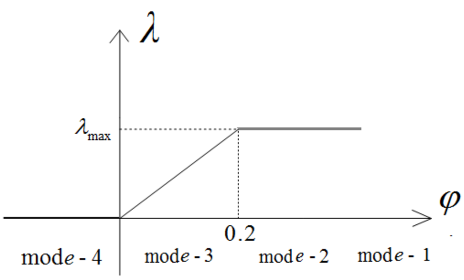

Figure 9. Model for parameter λ

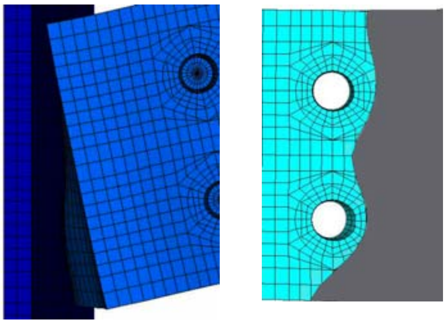

Figure 10. Separation characteristic in the web

$$B_a = B_r + B_{f1} + B_{f2}, \quad B_b = B_r + \alpha_{b1} B_{f1} + \alpha_{b2} B_{f2}, \quad B_c = B_r + \alpha_{c1} B_{f1} + \alpha_{c2} B_{f2}$$
$$\ell_b = g_2 - 0.5(B+t), \quad \ell_c = g_1 - 0.5B + (0.7+\lambda)t \qquad (3.4)$$

Bb and *Bc* are equivalent width of horizontal arm and vertical arm. Regarding to parameter λ, it can be taken as zero if bolt does not stretch and angle fails first.

It is observed from numerical results in Fig. 6 that when angle is thicker, bolt may have some small stretching and make contact separation curve pass bolt and reach the area behind bolt. This type of failure is mode 3 in Fig. 8. In general there are four types of connection failure modes as illustrated in Fig. 8. In order to achieve enough deformation ability in connection design, failure mode 1 and 2 should be avoided. Failure mode 4 is the best one. Therefore all studies conducted by authors of this paper are about how to do initial stiffness calculation on failure mode 4. Failure mode 3 has less capacity of deformation than mode 4, but much better than mode 1 and 2. Mode 3 is a possible true failure mode in structural design and should be included in initial stiffness investigation. This paper tries to modify existing stiffness calculation formula to cover both 4 and 3 failure modes. The strategy is to use yield strength difference between mode 4 and 3 to move contact separation curve towards rear edge of bolt head. When the difference (T4-T3) reaches 20% of T4, move the contact separation curve to the rear edge of bolt head. This will be extreme case. Based on all earlier reasoning, parameter λ calculation can be expressed as Eqn. 3.5. Fig. 9 shows the relationship between λ and φ. Let $\lambda = 0$ When $\varphi < 0$. *B* is the size of bolt head as indicated in Fig. 5.

$$\lambda = 5\varphi\left(\frac{B}{t} - 0.7\right), \qquad \varphi = (T_4 - T_3)/T_4 \qquad (3.5)$$

4. WEB ANGLE CONTRIBUTION AND STIFFNESS PREDICTION OF SPECIMENS

Fig. 10 shows web deformation and contact separation curve from finite element analysis. Although stress distribution of web is more complicated than top or seat angle, contact separation curve is still showing similar characteristics. Contact separation line around bolt is curve, not a straight line. The length of rigid segment is getting longer when it is away from rotation center. Considering that the bottom bolt has more contribution, length of rigid segment at bottom bolt is taken as ℓ_c in Eqn. 3.1. That means this will be the length of rigid segment for all other rigid segments. In Fig. 11, the contact area of web angle is divided into many small areas by bolts and resultant reaction force is assumed to be at bolt center. Then web tension stiffness contribution from each of areas can be calculated in a similar way used for top and seat angles using Eqn. 3.1 and 3.5.

Based on all assumption made above, for a semi-rigid connection with both flange angles (top and seat) and double web angles the rotational stiffness can be calculated in Eqn. 4.1. ℓ_i is the distance from bolt to the inflection point in flange angle.

$$K = \left[K_t(H+1.5t)(H+1.5t+\ell_i)\right] + \left[K_{t1}\ell_1^2 + K_{t2}\ell_2^2 + K_{t3}\ell_3^2\right] \tag{4.1}$$

$$\ell_i = \frac{(B_a/B_c)^{2/3}\ell_c^2}{(B_a/B_c)^{1/3}\ell_c + EB_a t^3 / 6K_s} \tag{4.2}$$

In order to verify the accuracy of initial stiffness prediction established in this study, all calculated results are compared with lab test results. In initial stiffness prediction using Eqn. 4.1, the first portion of Eqn. 4.1 is used for semi-rigid connections with top and seat angles. The second portion of Eqn. 4.1 is used for semi-rigid connections with double web angles. Fig. 12 shows all comparison between stiffness calculation using Eqn. 4.1 and lab test results. In the comparison of semi-rigid connections with top and seat angles, when bolt position parameter g_1 is higher, stiffness prediction tends to be higher. Stiffness prediction is lower when g_1 is smaller. All specimen shows difference less than 10%. For semi-rigid connections with double web angles, the highest stiffness connection is showing highest difference, about 20% higher. All other cases have difference within 10%.

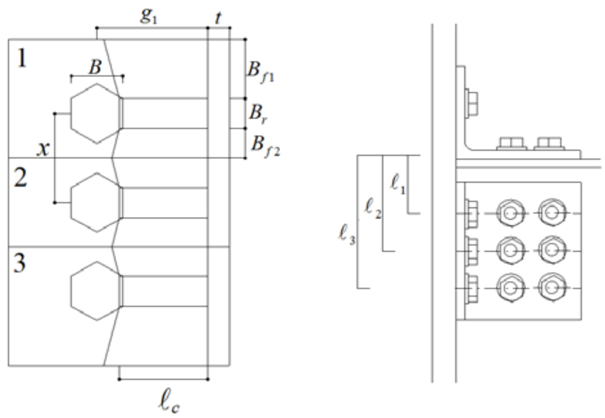

Figure 11. Segmental beam model for web angle

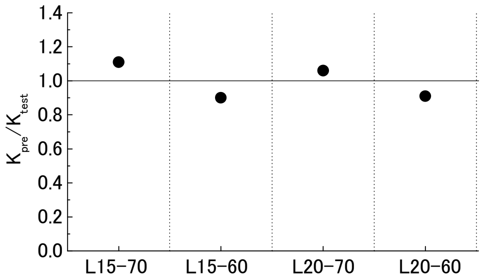

(a) Top and seat flange angle connection

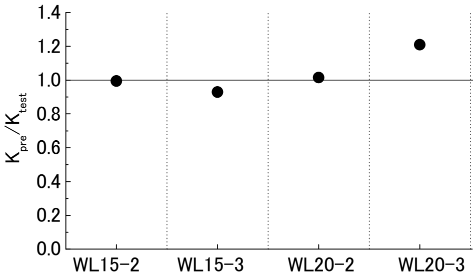

(b) Double web angle connection

Figure 12. Comparison of predicted initial stiffness with test results

5. CONCLUDING REMARKS

1) In order to improve stiffness prediction accuracy, this paper studies contact separation characteristic of flange angle and web angle and proposes new formula for correction factor calculation.

2) This paper modifies earlier stiffness calculation and makes calculation also valid for the connection where small deformation of bolt is expected.

3) This paper introduces a method to calculate web angle stiffness contribution.

4) 7 of 8 test results prove prediction error within 10% and only 1 test result shows 20% difference between prediction and test results.

REFERENCES

Lin, X.G. and Hamamoto, N. (2008). Prediction of Initial Stiffness of Semirigid Steel Beam-to-Column Connections with Bolts and Angles. *Proceedings of the 13th World Conference on Earthquake Engineering*, **Paper No.** 05-05-089.

Kishi, N. and Chen, W.F. (1990). Moment-rotation relations of semirigid connections with angles. *Journal of Structural Engineering.* **116:7**, 1813-1834.

Fealla, C., Piluso, V. and Rizzano, G. (1999). Structural Steel Semirigid Connections: Theory, Design and Software. CRC Press LLC, U.S.A.

Azizinamini, A., Bordburn, J.H. and Radziminski, J.B. (1987). Initial Stiffness of Semi-rigid Steel Beam-to-Column Connections. *Journal of Constructional Steel Research*. **No.8**, 71-90.

Lin, X.G. and Sugimoto, H. (2004). Experimental Study on Inelastic Behavior and Ultimate Strength of Steel Beam-to-Column Connections with Bolts and Angles. *Proceedings of the 13th World Conference on Earthquake Engineering*. **Paper No.** 1673.

Tanuma, Y. and Hashimoto, K. (1999). Moment-rotation behaviour of semirigid connections with angles. *Journal of Structural and Construction Engineering*. **No.515**, 123-130.

Tanaka, H. and Tanaka, A. (1975). Design formulas for the strength of t-stub connection. *Steel Construction Engineering*. **11:120**, 5-10.